IS THE HELLAS IMPACT RESPONSIBLE FOR EXTENSIONAL STRUCTURES AND VOLCANISM IN AND AROUND THE SOUTHERN HIGHLANDS OF MARS? T. Ruj[1], M. Kameyama[2], K. Kurosawa[3], K. Kawai[4], T. Usui[1], G. Komatsu[5]. [1]Institute of Space and Astronautical Science (ISAS), Japan Aerospace Exploration Agency (JAXA), 3-1-1 Yoshinodai, Sagamihara, Kanagawa 252–5210, Japan, (trishitruj@gmail.com), [2]Geodynamics Research Center, Ehime University, Ehime 790-8577, Japan, [3]Planetary Exploration Research Center, Chiba Institute of Technology, Chiba, Japan, [4]Department of Earth and Planetary Science, School of Science, University of Tokyo, Hongo 7-3-1, Bunkyo, Tokyo 113-0033, [5]International Research School of Planetary Sciences, Università d'Annunzio, Viale Pindaro 42, 65127, Pescara, Italy.

Introduction: In the context of the thermal evolution of Mars, the Hellas basin forming impact event was a huge contributor. It is the second biggest (after the SPA basin on Moon) impact structure preserved on the surface of the planetary bodies in the solar system. The huge bolide impact generated an enormous amount of heat at the bottom of the impact basin which could have altered the mantle dynamics for several millions of years.

The southern highlands region is heavily resurfaced by giant impact craters, such as Hellas, Argyre, Huygens, and Isidis [1–3], and their ejecta deposits. Noachian to Hesperian-aged volcanic plains are surrounded by the Noachian massive highland units [4]. In and around the Hellas basin and the surrounding region, we have observed a series of extensional structures (on the west and northwest) and a chain of volcanoes (in the northeast to southeast) (Figure 1). Most interestingly, the extensional structures and the chain of volcanoes have similar orientations and are of similar ages [5–7]. These observations of similarity in their orientations similarity and their similar ages intrigued us to explore the possibility of their genetic links with the Hellas impacts. Therefore, we assessed the possibility of the extensional structures and the volcanoes being related to the thermal heterogeneity caused by the Hellas basin forming bolide.

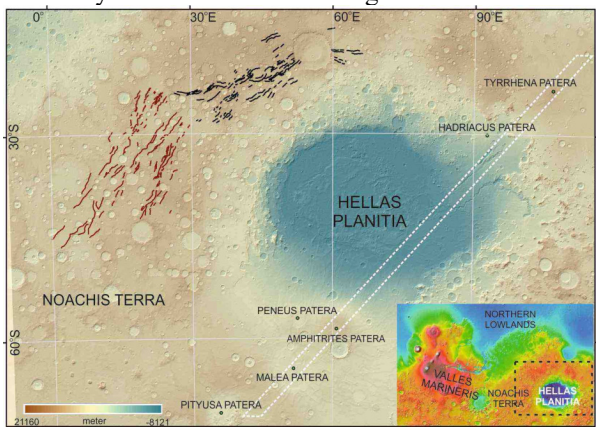

Figure 1: Mapped structures [1] overlaid on the MOLA-hillshade and MOLA DEM using 'Lambert Conformal Conic' projection. Red and black lines signify the Eastern Hellas Grabens (EHGs) and Northwestern Hellas Grabens (NWHGs). The dotted parallelogram (marked with white) on the eastern side of the Hellas basin shows a similar orientation trend of the circum Hellas Volcanics (CHVs). Global Martian colorized elevation map shows the area of interest in the dotted square.

Methodology and datasets: High-resolution images helped us to investigate the region in detail. We analyzed the general geology of the region with THEMIS-IR Day Global Mosaic (100 m/pixel) [8] and CTX imagery (6 m/pixel) [9]. We also used Mars Orbiter Laser Altimeter-High Resolution Spectral Camera (MOLA-HRSC) Digital Elevation Model (DEM) (200m/pixel) [10]. These images and the DEMs were incorporated into the ArcGIS platform for mapping and representation purposes.

We used impact simulations iSALE-2D shock physics code [11–15] and executed impact simulations of a spherical projectile over a flat surface to estimate the temperature distributions after a vertical impact. We ignored local topographic undulation as the crater basin is preserved on a southern highland crust and the effects of impact obliquity on the impact outcomes. In this simulation, we considered the size of the impactor (R_{imp}) as 200 km, and the impact velocity (V_{imp}) as 10 km/s. We used the ANEOS [16] for basalt [17] and dunite [18] to describe the martian crust and the martian mantle/the projectile, respectively. The "ROCK" strength model [12, 14] with the parameter sets for basalt [19] and dunite [20] was employed. We used Mars's lithospheric thickness to be 12 km, thermal gradient = 20 K/km, and crustal thickness = 65 km at the time of impact.

Then we input the results (the temperature distribution) to a time-dependent thermal convection of a fluid with an infinite Prandtl number and a temperature-dependent viscosity under the Boussinesq approximation in a cylinder. In this series of calculations, we imposed shallow asymmetries in the thickness of cold Thermal Boundary Layers (TBLs). In some of these calculations, we also imposed asymmetries in the shape of a hot and less viscous "bowl" mimicking an impact basin. But these asymmetries played a minor role. The impermeable and shear-stress-free conditions are adopted along all boundaries.

Results: Our results show that post-shock temperatures, T_{post} have been calculated by the ANEOS

(Figure 2). We obtained the enhanced temperature value up to ~700 km penetrating to the upper mantle of Mars.

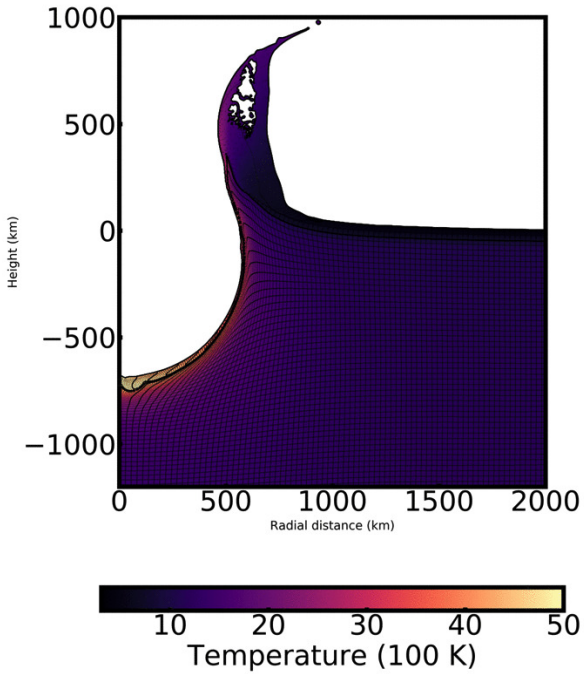

Figure 2: In the plane that includes the impact trajectory, at 5 t_s (is a characteristic time for projectile penetration and is defined to be $t_s = 2R_{imp}/V_{imp}$) for impact case (90°).

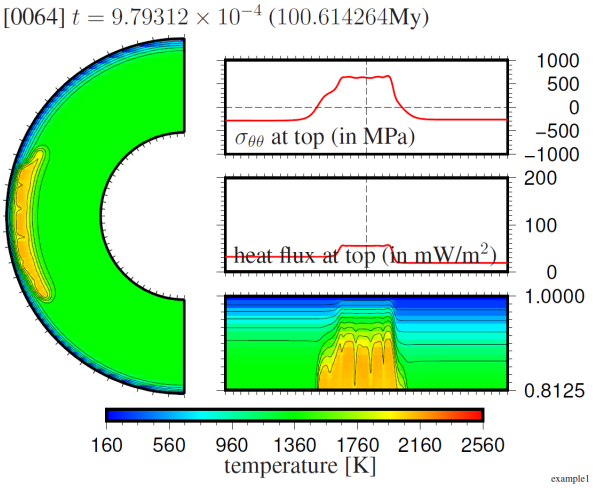

Figure 3: The occurrence of convective instabilities in the hot and less viscous "bowl" after 100 Ma of the impact. The asymmetries in the thickness of cold TBLs tend to enhance an onset of ascending flows near the edge of thinner TBLs.

In a series of our preliminary calculations, we found that a convective instability took place in a "bowl" of hot and less viscous domains in some cases where the cold TBLs are thick enough to confine the hot materials in the "bowl". By further imposing an asymmetry in the thickness of cold TBLs around the "bowl", an onset of ascending flows can be enhanced at the edges of the bowl associated with thinner TBLs (Figure 3).

Conclusion: These initial simulation results signify that the surrounding region might generate >500 MPa of positive stress (Figure 3, top right) which can be correlated with the series of extensional structures on the western part of the Hellas basin (Figure 1). On the other hand, the ascending flows (Figure 3, bottom right) can be correlated with the volcanisms in the northeastern to the southeastern region. This observation of probable mantle upwelling is supported by the presence of strong positive gravity anomalies along the volcanic centers [7,21], beneath the paterae. Now, the question comes why do we have such asymmetry on both sides of the crater? At this moment, we do not have a certain answer to this but there are several factors including oblique impact or dual impact [22], and differential crustal thickness at that time between either side might have influenced this scenario.

In the future, we are planning to answer the heterogeneity on both sides of the Hellas basin more in detail with the varying parameters.

Acknowledgments: This research was supported by JSPS KAKENHI 17H06459, and PRIUS research grant 2022-B02. We thank the developers of iSALE, including G. Collins, K. Wünnemann, B. Ivanov, J. Melosh, D. Elbeshausen, and T. Davison.

References: [1] Ruj, T. *et al.* (2017) J. *Maps 13*, 755–766. [2] Ruj, T. *et al.* (2022) *Remote Sens. 14*, 5664. [3] Tanaka, K.L. *et al.* (2014) *Planet. Space Sci. 95*, 11–24. [4] Platz, T. *et al.* (2013) *Icarus, 225*, 806–827. [5] Ruj, T. *et al.* (2019) *Geosci. Front. 10*, 1029–1037. [6] Williams, D.A. et al. (2009) *Planet. Space Sci. 57*, 895–916. [7] Williams, D.A. *et al.* (2010) *Earth Planet. Sci. Lett. 294*, 492–505. [8] Christensen, P.R. *et al.* (2004). *Space Sci. Rev., 110*, 85–130. [9] Malin, M.C. *et al.* (2007) *JGR Planets. 112*, E05S04. [10] Dickson, J.L. *et al.* (2018) *49th LPSC*, Abstract # 2480. [11] Elbeshausen, D. *et al.* (2009) *Icarus 204*, 716–731. [12] Collins, G.S. *et al.* (2004) *Meteorit. Planet. Sci. 39*, 217–231. [13] Amsden, A. *et al.* (1980) *Los Alamos National Laboratory (LANL) Technical Report.* [14] Ivanov, B.A. *et al.* (1997) *Int. J. Impact Eng. 20*, 411–430. [15] Wünnemann, K. *et al.* (2006) *Icarus 180*, 514–527. [16] Thompson, S. & Lauson, H. (1972) *SNL Report*, SC-RR-71 0714:113p. [17] Pierazzo, E. et al. (2005) *GSA special paper* 384, 443-457. [18] Benz, W. et al. (1989) *Icarus* 81, 113-131. [19] Ivanov, B. A. et al. (2010) GSA special paper 465, 29-49. [20] Johnson, B. C. et al. (2015) Nature 517, 339-341. [21] Genova, A. *et al.* (2016) *Icarus 272*, 228–245. [22] Komatsu, G. *et al.* (2017) *48th LPSC*, Abstract # 1964.